FONDATION SINGER-POLIGNAC

PHYSIOLOGICAL CONSEQUENCES OF ACh RECEPTOR AND ESTERASE DISTRIBUTION IN VERTEBRATE ENDPLATES

by

Miriam M. SALPETER and Bruce R. LAND

EXTRAIT DE

LA TRANSMISSION NEUROMUSCULAIRE.
LES MÉDIATEURS ET LE « MILIEU INTÉRIEUR »

MASSON, 1980

6

PHYSIOLOGICAL CONSEQUENCES OF ACh RECEPTOR AND ESTERASE DISTRIBUTION IN VERTEBRATE ENDPLATES

by

Miriam M. SALPETER and Bruce R. LAND *

In our talk this afternoon, we will first summarize briefly the work from our laboratory over the past 10 years in which we used quantitative EM autoradiography to assess the localization and concentrations of acetylcholine esterases (AChE) and receptors (AChR) at various vertebrate neuromuscular junctions (nmj). These studies have led us to speculate that a quantum of ACh can interact with a very small postsynaptic area at saturating ACh concentrations (Fertuck and Salpeter, 1976; Matthews-Bellinger and Salpeter, 1978). This geometric model, which we will call the « saturated disc » model, has certain physiological consequences that will be discussed in the second part of this talk. Thirdly, we will tell you about some recent experiments being conducted in our laboratory (in collaboration with Edwin Salpeter) designed to evaluate the saturated disc model.

The quantitative assessment of AChE and AChR distribution at nmj's required the development of autoradiographic procedures which are reproducible and easily calibrated. We will not go into the technical details of our « flat substrate » specimen which we developed for this purpose, since it has been described fully in earlier publications (*e. g.* Salpeter and Bachmann 1964, 1972), and since it has now become routine for similar studies in other laboratories (*e. g.* Porter and Barnard, 1975; Bourgeois *et al.*, 1978). We have calibrated this specimen for sensitivity, *i. e.* determining the number of radioactive decays which give, on the average, one developed grain (Bachmann and Salpeter, 1967; Salpeter and Szabo, 1972; Fertuck and Salpeter, 1974); and for resolution, *i. e.* determining the distribution of developed

* Section of Neurobiology and Behavior and Department of Applied Physics, Cornell University, Ithaca, N. Y., U. S. A. Supported by a Postdoctoral Fellowship from Muscular Dystrophy Association (BRL) and by a grant from NIH.NS 09315.

grains expected from various defined radioactive sources in a tissue (Salpeter *et al.*, 1969, 1977 and 1978 *a*). Using these calibrations we are able to locate labeled structures (within 500 to 1,500 Å resolution; depending on the isotope and photographic conditions) and establish how many labeled molecules are present per unit area or volume of that structure.

Figure 1 shows an EM autoradiogram of a mouse nmj whose AChE's were labeled with ^{3}H-diisopropylfluorophosphate (^{3}H-DFP) using appropriate controls to avoid labeling non-specific esterases (Rogers *et al.*, 1969). The grains are seen in a band overlying the post-junctionnal folded membrane (pjm). (The resolution is 1,500 Å under these conditions with Ilford L_4 emulsion, Salpeter *et al.*, 1969). Figure 2 is an EM autoradiogram of a lizard nmj whose AChR's were labeled with ^{125} I-α-bungarotoxin (^{125}I-α-BGT) (resolution = 800 Å under these conditions with Ilford L_4 emulsion, Salpeter *et al.*, 1977). The grains are concentrated at the top ~ 2,000 Å of the (pjm) overlying a region of thickened post junctional membrane (tpjm). Figure 3 is a schematic drawing of a mouse nmj with a histogram on either side. The one on the right represents the distribution of developed grains due to ^{3}H-DFP and thus labeled AChE sites (see Salpeter, 1969; Salpeter *et al.*, 1972) whereas the one on the left represents the distribution of developed grains due to ^{125}I-α-BGT and thus labeled AChR sites (Fertuck and Salpeter, 1976). Note

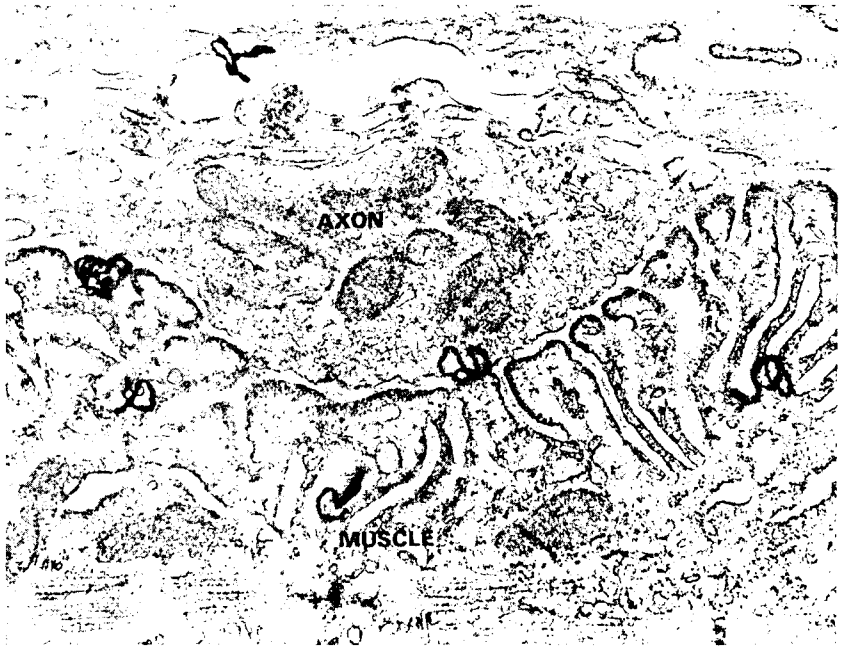

FIG. 1. — *EM autoradiogram of mouse neuromuscular junction in which AChE sites are labeled with* ^{3}H-*DFP*. Emulsion: Ilford L_4, Developer: D19, Resolution: (HD) 1,500 Å. Developed grains are distributed over region of post-junctional folded membrane (× 20,800) (We thank Dr. Hedwig KASPRZAK for this picture).

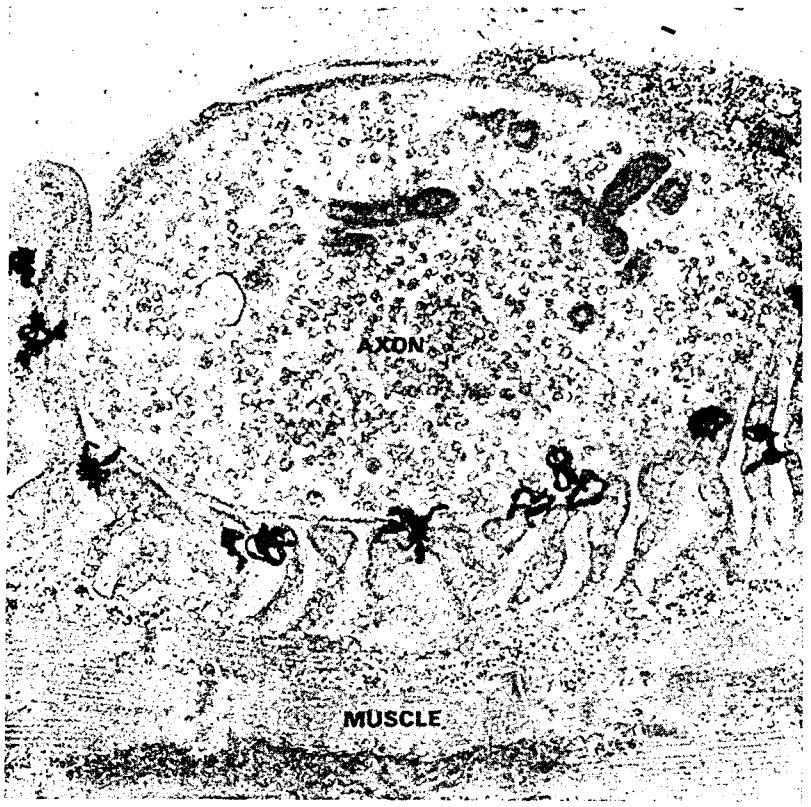

FIG. 2. — *EM autoradiogram of lizard neuromuscular junction whose AChR sites are labeled with* ^{125}I-α-*BGT*. Emulsion: Ilford L_4, Developer: D19, Resolution: (HD) 800 Å. Developed grains are concentrated at top of the post junctional membrane (· 20,800).

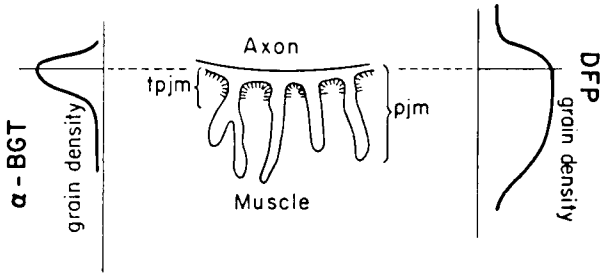

FIG. 3. — *Schematic drawing of mouse neuromuscular junction with histograms representing grain distributions due to* ^{3}H-*DFP label (right) and* ^{125}I-α-*BGT label (left)*. The distribution after ^{3}H-DFP is what would be expected from labeled sites along the post junctional membrane (pjm) down to the bottom of the ~ 8,000 Å deep folds. The grain distribution after ^{125}I-α-BGT is what would be expected from labeled sites concentrated along the thickened top ~ 2,000 Å of the pjm.

that we use the term AChR (or R) synonymously with one ACh binding site or one α-BGT binding site.

Quantitation of the AChE and R sites shows that the AChE is present at a concentration of ~ 2,500 ± 500 sites/μ^2 of pjm surface area *. The receptor on the other hand is present at a concentration of ~ 20,000 ** ± 8,000 sites/μ^2 of specialized dense membrane at the top of the pjm. The receptor of thus present in a 5-10 fold higher concentration than esterases at the top of the pjm whereas the esterases exceed receptor at the bottom of folds. The organization appears similar in frog (Matthews-Bellinger and Salpeter, 1978) and lizard muscle (Land *et al.*, unpublished) as that previously seen in the mouse.

This distribution of AChE and AChR has led us to suggest the « saturated disc » model. It is based at present on the qualitative argument that a quantal packet of ACh (~ 10^4 ACh molecules; see Kuffler and Yoshikami, 1975) need not diffuse very far from its site of release before it can see a postsynaptic area containing a number of ACh binding sites equal to the number of ACh molecules in the quantum. (At 20,000 sites/μm^2, 10,000 binding sites occupies ~ 0.5 μm^2). We will call this the quantal area (Aq). If binding were fast enough, an ACh quantal packet could be fully bound within this small area and thus, during most of its brief free life-time, the ACh will act at very high concentrations. We calculate that this ACh concentration could be on the average ~ 10^{-3} M, and thus more than 10 times higher than even the highest equilibrium dissociation constants reported for ACh binding to either esterase (Rosenberry, 1975) or receptor (*e. g.* Dreyer and Peper, 1975; Sheridan and Lester, 1977)

We do not of course know the exact binding time for ACh to AChR and therefore are not able to define the actual area (to be called Ae) which is seen by a quantum of ACh. The upper limit to Ae was given on physiological grounds by Hartzell *et al.*, 1975, as < 4 μ. We expect that Ae is closer to Aq than this upper limit suggests, and are currently engaged in studies to determine these limits more precisely.

A plausibility argument in favor of this suggestion is based on the physiological consequences of inactivating AChE at the nmj's. Hartzell *et al.* (1975), and others have shown that inactivating AChE produces at most a 20 % increase in the miniature endplate current (mepc) amplitude. Yet, as stated above *; the AChE is believed to reside in the basal lamina of the clefts. A persistent question therefore was how the ACh could run the grauntlet of AChE on its way to the receptor, and yet remain so little affected. However the « saturated disc » model would predict just that. We have shown that

* Evidence from other laboratories have established that the esterases are localized within the basal lamina of the clefts (Hall and Kelley, 1971; Betz and Sackmann, 1973; McMahan *et al.*, 1978). Combining these studies with our own data (Salpeter *et al.*, 1978 *b*) we suggest that the esterases are located in a sheet of basal lamina overlying the surface contours of the pjm.

** Our previously published value of 30,000 ± 30 % has to be corrected down by ~ 25 % due to some uncorrected systematic factors.

within the receptor area (Aq) AChR outnumbers AChE ~ 8 to 1. Thus if the released ACh acted over an area Ae which is not much larger than Aq, then during the 60-100 μsec of the mepc rise time, about 20 % of the packet could bind to, and saturate the available AChE (occupancy time of ACh on AChE is ~ 100 μsec, Wilson and Harrison, 1961 and Rosenberry, 1975), while the remaining ~ 80 % of ACh can interact with receptors. By the time the ACh leaves the receptor (AChR occupancy time on receptor is ~ 1 msec if it equals channel open time, Katz and Miledi, 1973 *b*), the AChE will again be free to hydrolyse it. A consequence of this reasoning would be that AChE inhibitors should then make only ~ 10-20 % more ACh available for binding to receptor and thus at most increase the time to peak and amplitude of a mepc by this trivial amount. This is indeed what Hartzell *et al.* (1975) have shown, and we have confirmed in preliminary unpublished studies. Of course during the decaying phase of the mepc in the absence of AChE, the ACh can bind repeatedly to AChR and consequently the decay time of a mepc is lengthened considerably (Katz and Miledi, 1973 *a*). The model predicts that as AChR site density is decreased, the effect of inactivating AChE on mepc amplitude and time to peak should be greater.

We want now to describe some recent experiments (in collaboration with E. Salpeter) aimed at defining the parameters of the « saturated disc » model more quantitatively. The first of these involves testing what happens to the time to peak, and amplitude of a mepc when the receptor site density (σ) is lowered in an esterase inactivated endplate. We are thereby able to distinguish those factors which depend on σ (*e. g.* diffusion and binding-half life of an ACh molecule) from those that do not (*e. g.* conformational change time to open ion gates). We used the lizard intercostal muscle since the compact endplates are much smaller than the electrical length constant and thus may be uniformly clamped. The muscle is thin (one to two fiber layers thick) allowing easy visualization of the endplates with Hoffman modulation optics. The AChE's are inactivated by DFP (1 mM for 20 min). The AChR site density is left normal or is decreased with α-BGT (4×10^{-8} M for either 20 or 40 min). The muscles are voltage clamped at 100 mV and 23° C using 3-6 megohm electrodes. Clamp output data is passed through a 2-pole Butterworth filter with 4kHz cut-off. Approximately 200 mepcs are obtained from each fiber. For each mepc, computer smoothing is used to find both the half rise time, and the amplitude. Mepc's are then superimposed to match the half rise-time point, and the raw data averaged to improve the signal-to-noise ratio. After the physiological recordings are complete the muscles are incubated in ^{125}I-α-BGT (5×10^{-7} M for 2 hours), fixed in glutaraldehyde and formaldehyde as described for the frog (Matthews-Bellinger and Salpeter, 1978), and prepared for EM autoradiography.

Figure 4 shows some voltage clamp traces of mepcs at different degrees of α-BGT poisoning. We see that in the esterase inactivated endplate the amplitude decreases and the time to peak lengthens after α-BGT treatment. Figure 5 shows two averaged traces: one of unusually low amplitude for a normal preparation and the second of an unusually high amplitude for a

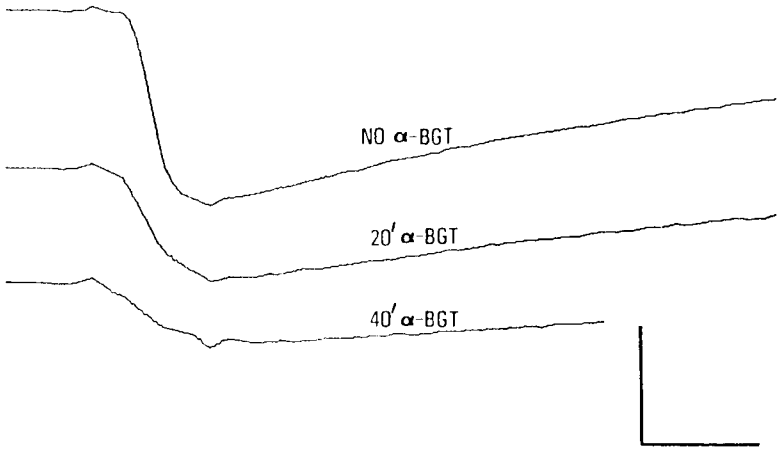

FIG. 4. — *Computer averaged traces of m pcs from esterase inactivated, voltage clamped lizard neuromuscular junctions.* The top ' ce is an average from preparations not treated with α-BGT, the middle and bottom t. es are from preparations treated for 20 min and 40 min respectively in 4 × 10 ⁻⁸ M α-BGT. Note increase in time to peak and decrease of amplitude with increasing inactivation. ne scale is 5 nA vertically and 0.4 msec horizontally.

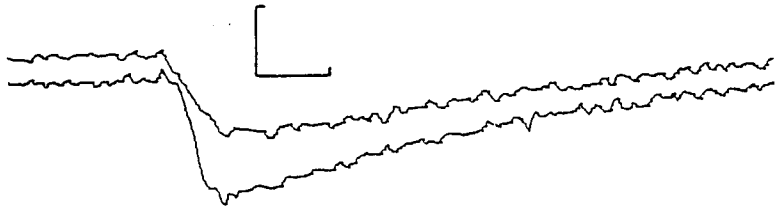

FIG. 5. — *Two averaged traces of mepcs of approximately equal amplitude.* Top trace is from among the largest of heavily α-BGT inactivated endplates (40 min) and bottom trace is from among smallest of α-BGT untreated endplates. Note the longer time to peak in mepc from α-BGT treated endplate. This shows that the lengthening in the time to peak after AChR inactivation is not an artefact of the averaging procedure of meeps with low signal-to-noise ratio. Scale: 3 nA vertically and 0.5 msec horizontally.

poisoned preparation. The two have similar absolute amplitudes and yet very different rise times. This shows that the increasing mean rise time with decreasing σ is not an artifact of the averaging process when the signal-to-noise ratio is low. We plotted the correlations between AChR site density and time to peak (fig. 6) and amplitude (fig. 7) of the mepcs.

The rise time of a mepcs is determined by 3 factors: the time (t_d) for ACh to diffuse from its site of release to the receptor; the time (t_b) for ACh to bind to the receptor (*i. e.* the half life of the free ACh); and some constant delay times (t_c) between ACh release and the initiation of ion flux across the postsynaptic membrane. To analyse these studies we note that t_d is inversely

FIG. 6. — *Mepc rise time (20-80 %) versus $1/\sigma$ correlation.* Vertical error bars represent the standard deviation of the rise times. Horizontal error bars represent the coun-t ing uncertainly in the autoradiographic process plus intersample variations in site density.

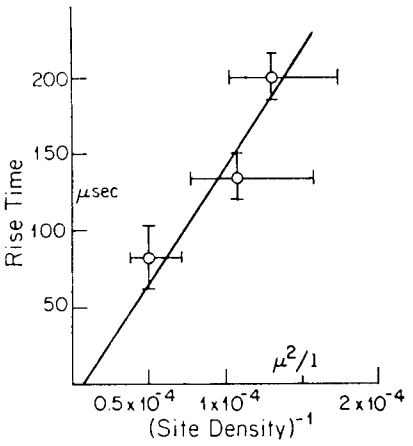

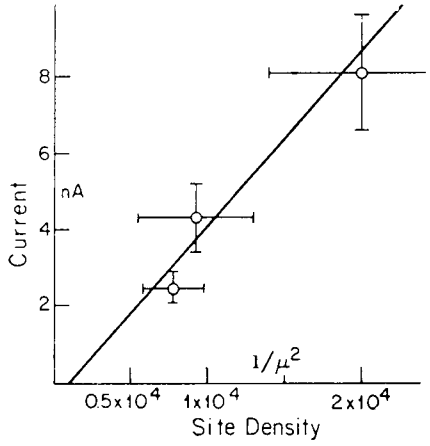

FIG. 7. — *Mepc amplitude versus σ correlation.* Vertical error bars represent the 1/2 width of the composite distribution of amplitudes for all cells of a given α-BGT inactivation level. Horizontal error bars are as given in figure 6.

proportional to the area covered (and thus to σ) and that t_b is inversely proportional to the concentration of reactants (and thus again to σ). On the other hand, t_c, a time delay, *e. g.* the time to open ion channels once the ACh is bound to receptor, must be independent of σ. Figure 6 shows that the time to peak is proportional to $1/\sigma$ as is expected if the time to peak were controlled by t_d and t_b and if t_c was negligible *. This is consistent with the conclusions reached by Sheridan and Lester (1977).

The fact that the time to peak continues to lengthen proportionally to $1/\sigma$ over the entire range of σ's tested, suggests that the ACh is still equally effective in opening channels, even though the reduced σ requires the ACh to spread over a larger ($\sim$ 3 fold) area to see an equal number of receptors.

Figure 7 shows that the mepc amplitude is proportional to σ. This relation is compatible with a model which assumes that there are 2 ACh (or α-BGT)

* Note added in proof : Newer data now suggests a small measurable value for t_c, on the y-intercept in fig. 6 (Land, Salpeter and Salpeter, PNAS, 1980, in press).

binding sites (R) per ACh receptor-channel complex (R_c) and that both must be occupied by ACh (A) to give an open channel (R_c^*). (Binding to one site does not effect the binding to the other site).

$$i.\ e. \qquad 2A + R_c \rightarrow A + AR_c \rightarrow A_2R_c^*$$

Table I. — Consequences of α-BGT on the relative effectiveness of ACh in opening ion channels

*Occupancy of R_c **	*For n = 1*		*For n = 2*	
	ACh effective	*ACh wasted*	*ACh effective*	*ACh wasted*
1. AR AR	2	0	2	0
2. BR AR	1	1	0	1
3. AR BR	1	1	0	1
4. BR BR	0	2	0	0

Where n = Number of binding sites per R_c
R_c = ACh receptor channel complex
R = ACh binding site
A = ACh
B = α-bungarotoxin (α-BGT)
σ = R/μm^2 not occupied by B

* As long as ACh concentration is high enough, all the ACh molecules of a quantum will eventually bind to R's even though they have to spread over a larger area as σ is decreased. Thus the relative decrease in mepc amplitude is proportional to the relative number of ACh molecules wasted on partially α-BGT inactivated receptor complexes (*i. e.* conditions 2 and 3 for $n = 2$).

This argument, summarized in table I, depends on the claim we just made (based on figure 6) that most of the ACh packet is at saturating concentrations during the rise time of a mepc and thus eventually bound to receptor. As σ is decreased the ACh spread over a larger area to bind. The time to peak can lengthen as seen in figure 6. However if there were only one binding site (R) per receptor channel complex, (R_c), then even though the ACh would have to spread farther before binding an unoccupied binding site (R), once bound, each ACh molecule should be equally effective in opening the ion gate. Thus one would expect that initially, until ACh is lost out of the cleft or the concentration becomes too diluted to bind effectively, the amplitude should remain constant. This would predict that after α-BGT incubation the mepc amplitude should be independent of σ. However if there were 2 binding sites per R_c, and both needed to be occupied in order to open the channel, then whenever only one of the 2 sites were occupied by α-BGT, an ACh could still bind to the other site but not be effective in opening a channel, and thus be wasted. Quantitatively one finds that, if n binding sites are required to open an ion gate and if one assumes the absence of cooperativity in binding, the amplitude should then be proportional to σ^{n-1}. Our results are therefore comparable with $n = 2$ (see also Adams and Sakmann, 1978).

We are now engaged in studies to determine the relative effects of t_a and t_b on the time course of the mepc, and the effect of esterase inactivation on mepc amplitude and time to peak. These studies should allow us to define more precisely the actual area fo Ae and determine the limits to the « saturated disc » model.

Bibliography

Adams (P. R.) and Sackmann (B.), 1978. — Agonist-triggered endplate channel opening. *Biophy. J.*, **21**, 53 *a*.

Bachmann (L.) and Salpeter (M. M.), 1967. — Absolute sensitivity of electron microscope autoradiography. *J. Cell Biol.*, **33**, 299-305.

Betz (W.) and Sackmann (B.), 1973. — Effects of proteolytic enzymes on function and structure of frog neuromuscular junctions. *J. of Physio.* (Lon.), **230**, 673-688.

Bourgeois (J. P.), Popot (J. L.), Ryter (A.) and Changeux (J. P.), 1978. — Quantitative studies on the localization of the cholinergic receptor protein in the normal and denervated electroplaque from electrophorus electricus. *J. Cell Biol.*, **79**, 200-216.

Dreyer (F.) and Peper (K.), 1975. — Density and dose-response curve of acetylcholine receptors in frog neuromuscular junction. *Nature* (Lon.), **253**, 641-643.

Fertuck (H.) and Salpeter (M. M.), 1974. — Sensitivity in electron microscope autoradiography for I^{125}. *J. Histochem. Cytochem.*, **22**, 80-87.

Fertuck (H.) and Salpeter (M. M.), 1976. — Quantitation and junctional and extrajunctional acetylcholine receptors by electron microscope autoradiography after ^{125}I-α-bungarotoxin binding at mouse neuromuscular junctions. *J. Cell Biol.*, **69**, 144-158.

Hall (Z.) and Kelley (R. B.), 1971. — Enzymatic detachment of endplate acetylcholinesterase from muscle. *Nature New Biol.*, **232**, 62-63.

Hartzell (H.), Kuffler (S.) and Yoshikami (D.), 1975. — Post-synaptic potentiation: interaction between quanta of acetylcholine at the skeletal neuromuscular synapse. *J. Physiol.*, **251**, 427-463.

Katz (B.) and Miledi (R.), 1973 *a*. — The binding of acetylcholine to receptors and its removal from the synaptic cleft. *J. Physiol.*, **231**, 549-574.

Katz (B.) and Miledi (R.), 1973 *b*. — The characteristics of « end-plate noise » 7 produced by different depolarizing drugs. *J. Physiol.*, **230**, 707-717.

Kuffler (S. W.) and Yoshikami (D.), 1975. — The number of transmitter molecules in a quantum: an estimate from iontophoretic application of acetylcholine at the neuromuscular synapse. *J. Physiol.*, **251**, 465-482.

Matthews-Bellinger (J.) and Salpeter (M. M.), 1978. — Distribution of acetylcholine receptors at frog neuromuscular junctions with a discussion of some physiological implications. *J. Physiol.*, **279**, 197-213.

McMahan (U. J.), Sanes (J. R.) and Marshall (L. M.), 1978. — Cholinesterase is associated with the basal lamina at the neuromuscular junction. *Nature* (Lon.), **271**, 172-174.

Porter (C. W.) and Barnard (E. A.), 1975. — The density of cholinergic receptors at the endplate post-synaptic membrane: ultrastructural studies in two mammalian species. *J. Memb. Biol.*, **20**, 31-49.

Rogers (A. W.), Darzynkiewicz (Z.), Salpeter (M. M.), Ostrowski (K.) and Barnard (E. A.), 1969. — Quantitative studies on enzymes in structures in striated muscles by labeled inhibitor methods. I. The number of acetylcholinesterase molecules and of other DFP reactive sites at motor endplates, measured by radioautography. *J. Cell Biol.*, **41**, 665-685.

ROSENBERRY (J.), 1975. — Acetylcholinesterase. *Adv. in Enzymol.*, **43**, 103-218.

SALPETER (M. M.), 1969. — Electron microscope radioautography as a quantitative tool in enzyme cytochemistry. II. The distribution of DFP-reactive sites at motor endplates of a vertebrate twitch muscle. *J. Cell Biol.*, **42**, 122-134.

SALPETER (M. M.) and BACHMANN (L.), 1964. — Autoradiography with the electron microscope, a procedure for improving resolution, sensitivity and contrast. *J. Cell Biol.*, **22**, 469-477.

SALPETER (M. M.) and BACHMANN (L.), 1972. — Autoradiography in *Principles and techniques of electron microscopy, biological applications*. Ed. M. A. Hayat. Van Nostrand Reinhold, New York, vol. **2**, 221-278.

SALPETER (M. M.), BACHMANN (L.) and SALPETER (E. E.), 1969. — Resolution in EM radioautography. *J. Cell Biol.*, **41**, 1-20.

SALPETER (M. M.), PLATTNER (H.) and ROGERS (A. W.), 1972. — Quantitative assay of esterases in end plates of mouse diaphragm by electron microscope autoradiography. *J. Histochem. Cytochem.*, **20**, 1059-1068.

SALPETER (M. M.) and SZABO (M.), 1972. — Sensitivity in electron microscope autoradiography. I. The effect of radiation dose. *J. Histochem. Cytochem.*, **20**, 425-434.

SALPETER (M. M.), FERTUCK (H. C.) and SALPETER (E. E.), 1977. — Resolution in electron microscope autoradiography. III. Iodine-125, the effect of heavy metal staining and a reassessment of critical parameters. *J. Cell Biol.*, **72**, 161-173.

SALPETER (M. M.), MCHENRY (F. A.) and SALPETER (E. E.), 1978 *a*. — Resolution in electron microscope autoradiography. IV. Application to analysis of autoradiograms. *J. Cell Biol.*, **76**, 127-145.

SALPETER (M. M.), ROGERS (A. W.), KASPRZAK (H.) and MCHENRY (F. A.), 1978 *b*. — Acetylcholinesterase in the fast extraocular muscle of the mouse by light and electron microscope autoradiography. *J. Cell Biol.*, **78**, 274-285.

SHERIDAN (R. E.) and LESTER (H. A.), 1977. — Rates and equilibria at the acetylcholine receptor of electrophorus electroplax. *J. Gen. Physiol.*, **70**, 187-219.

WILSON (I. W.) and HARRISON (M. A.), 1961. — Turnover number of acetylcholinesterase. *J. Biol. Chem.*, **236**, 2292-2295.